

HOLISTIC DESIGN OPTIMIZATION OF THE PV MODULE FRAME: CTM, FEM, COO AND LCA ANALYSIS

Ammar Tummali^{1,2}, Andreas J. Beinert¹, Christian Reichel¹, Max Mittag¹, Holger Neuhaus¹

¹Fraunhofer Institute for Solar Energy Systems ISE, Heidenhofstrasse 2, 79110 Freiburg, Germany

²University of Freiburg, IMTEK, Georges-Koehler-Allee 103, 79110 Freiburg, Germany

ABSTRACT: We present a holistic approach for the photovoltaic (PV) module frame optimization that considers technical as well as economic and ecological aspects for different frame designs. This provides insights into a method to reduce frame costs and carbon footprint without compromising mechanical stability as well as module power. Finite element method (FEM) simulations of module and frame are used to assess mechanical stability, cell-to-module (CTM) analysis is used to evaluate power losses affected by frame overlap, a bottom-up cost model is used for the economic analysis of material and process cost shares of frame manufacturing, and a life cycle assessment (LCA) analysis is applied to evaluate the ecological footprint ($\text{CO}_{2\text{-eq}}/\text{kW}_\text{P}$). Compared to a reference frame, the exemplary optimized frame design shows 2.6% less deflection, which corresponds to around 0.7 mm. CTM results show that a bigger frame width lightly decreases the cover coupling power gain. By increasing the front frame width from 16 mm to 20 mm the module power is reduced by 0.12 Wp. Cost analysis suggests that the optimized frame can save around 30 g aluminum which reduces the module cost by 0.1%. LCA results are directly correlated to the material mass of the corresponding design. Results show that using the optimized frame can save 0.8 kg $\text{CO}_{2\text{-eq}}/\text{kW}_\text{P}$ due to the saving in aluminum compared to the reference frame.

Keywords: CTM, FEM, LCA, COO, Frame, PV module, Optimization, Simulation

1. Introduction

As PV technologies evolve rapidly, the PV market expands and becomes more complex with all components of the module being permanently optimized [1, 2]. One of these components is the aluminum frame, which on the one hand is an important structural component of the module and provides the required mechanical stability, and on the other hand affects the performance and overall cost of the PV module.

An analysis of more than 250 technical datasheets of PV modules from 1995 to 2020 shows the historical evolution of the module frame dimensions, where for example the frame height h_{frame} was reduced from 50 mm to 35 mm in the last 30 years.

The frame dimensions play a crucial role in a holistic optimization as frame height and width which are closely related to the necessary aluminum amount, which is related to costs, environmental impact, as well as indirectly to the mechanical stability and electrical performance.

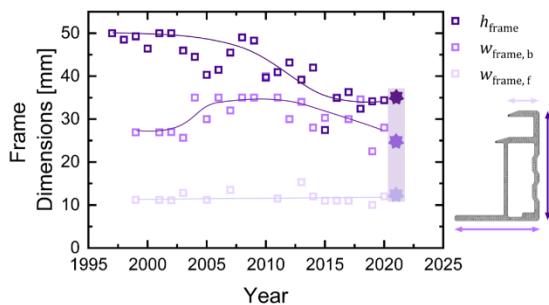


Figure 1: Historic trend of the frame dimensions, including frame height h_{frame} (dark purple), front frame width $w_{\text{frame},f}$ (purple) and frame base width $w_{\text{frame},b}$ (light purple). The corresponding lines are guide-to-the-eyes. Dimensions of the reference frame (stars) are marked in purple.

Here, we represent an approach for a holistic PV module frame optimization. Within this study we investigate and optimize exemplary PV module frame design based on mechanical, electrical, economic, and

environmental analysis. Concerning the mechanical analysis, previous studies [3–6] investigated the module deformation and stress distribution under mechanical pressure loads. As related previous work studies the mechanical stress of solar cells [7] we propose an approach to optimize the module frame design and apply FEM simulations on the PV module including the aluminum frame with various designs to define the module maximum deflection under 2400 Pa push load according to the IEC 61215 standard. Changing the frame design also affects the geometry of the module and its light-exposed internal areas which have impact on the loss and gain channels in the PV module. For this purpose, we complement the models in a previous related work [8], where loss and gain mechanisms in the PV module are investigated using CTM analysis. Additionally, the module frame forms about 9–12% of the whole module cost [9, 10], which highlights the importance of the design optimization. Therefore, we study the impact of the frame design on the cost of ownership (COO). Lastly, most frames are made of aluminum, which is an energy-intensive material and may significantly contribute to a higher carbon footprint [11–14]. This aspect is investigated by applying detailed LCA analysis. All previous aspects enlarge the importance of optimizing the frame design and finding a balance point between its mechanical, electrical, economic, and ecologic impact. The Approach and results presented in this paper are based on detailed work in [15].

2. Method

We parameterize the frame design and define variables that affect the PV module mechanically and electrically and influence the amount of aluminum used. Relevant parameters that affect the different aspects considered in this study are illustrated in Figure 2. Like common PV module designs, we assume that the rear side frame width $w_{\text{frame},r}$ is equal or bigger than the front frame width $w_{\text{frame},f}$ with a fixed frame thickness t_{frame} of 1.8 mm and rubber seal thickness t_{rubber} of 2 mm. Furthermore, we ensure that the distance through insulation d_{li} between the string connector and the aluminum frame conform to the standard IEC 61730 which is approximately 21 mm for class II PV modules. We set different sets of front and rear

frame widths shown in Table 1 to specify a wide realistic and reasonable range of the different frame parameters including standard and most common frame parameters. The cross-section of studied frame designs is shown in Figure 3 and the overlap is calculated using Equation 1:

$$W_{\text{overlap}} = W_{\text{frame}} - t_{\text{frame}} - t_{\text{rubber}} \quad (\text{Eq. 1})$$

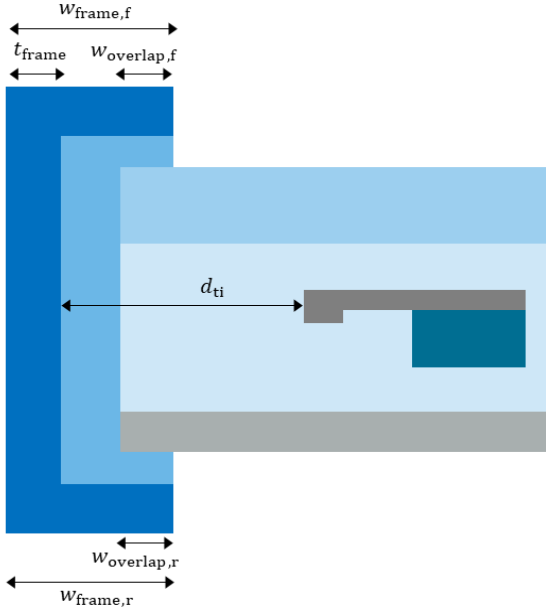


Figure 2: Module layer structure and parameters for frame description.

Table 1: Frame parameters used in the simulations. Reference frame values are sprinted in italic purple.

Front frame width $W_{\text{frame},f}$ [mm]	Rear frame width $W_{\text{frame},r}$ [mm]
10	12
12	14
14	16
<u>16</u>	18
18	<u>20</u>

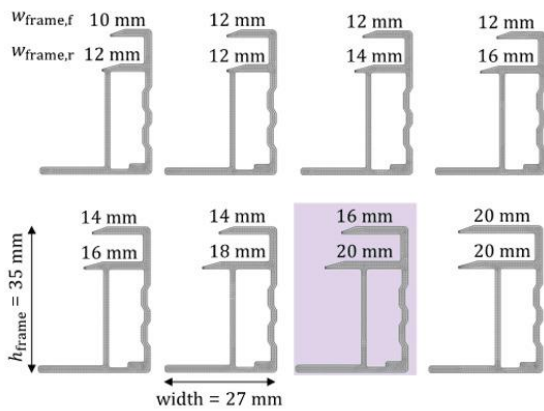


Figure 3: Cross-section of exemplary frame designs with the mesh used in the FEM simulations. Reference frame is marked in purple.

As reference module for the comparison in our study, we choose standard frame parameters of 16 mm front width and 20 mm rear width. After calculating the relevant

frame parameters, we use them to define different sets of combinations to represent different frame designs variants for the FEM analysis. In a first step, we simulate the deflection at 2400 Pa push load for the different frame geometries with the parameters in Table 1. Afterwards, CTM, COO and LCA analyses are carried out to simulate the impact on the electrical output of the module, cost, and global warming potential. Table 2 and Table 3 show the solar cell parameters and the used module components in the simulation. The simulated PV module is a 120 M6 half-cells glass-backsheet module with laminate dimensions of $1.76 \times 1.05 \text{ m}^2$.

Table 2: Solar cell parameters used in the simulations.

Solar Cell	
Format	5 busbar M6 half cell (83×166 mm)
Power	3.10 W

Table 3: Module parameters used in the simulations.

Solar Module	
Laminate Length	1.67 m
Laminate Width	1.05 m
Glass Thickness	3.2 mm AR-coated glass
Encapsulation	2×0.45 mm EVA
Backsheet	0.218 mm white backsheet

2.1. Mechanical Analysis

For the mechanical analysis, we adapt FEM models from previous studies [3, 16] to the investigated PV module topology. The fully parameterized frame is considered in full detail, as depicted in Figure 4. The attachment to the PV laminate is realized by silicone adhesive. For a more detailed description of the FEM model as well as the material properties, we refer to [3]. We simulate the lamination process prior to the mechanical push load according to the IEC 61215 standard. As an improvement to the previously published FEM models, the geometric non-linearity of the deflection is considered in the static simulation as well as the contact to the mounting rail. The module clamp is simulated by a weak constraint, which suppresses the displacement in z-direction on the outer edge of the frame, as depicted in Figure 4 by the purple line. For each frame design using the parameters in Table 1 we evaluate the maximum deflection d_{max} at 2400 Pa push load.

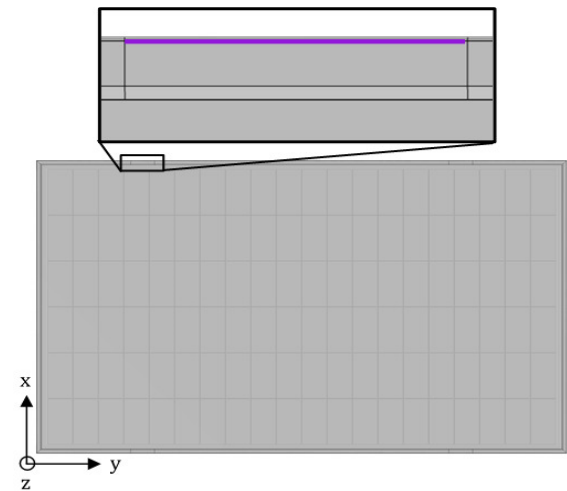


Figure 4: Module topology as modelled in the FEM analysis with the weak constraint on the frame edge (purple line) simulating the frame clamp.

2.2. Cell-To-Module (CTM) Analysis

The CTM simulation is done at standard test conditions (STC) on a 120 M6 monofacial half-cells glass-backsheet PV module with different frame designs as presented above. The models are based on a bottom-up multi-physics approach and are integrated into a consistent framework that allows the direct comparison of different module designs [17–19]. Using the CTM analysis we evaluate the impact of frame design on the loss and gain mechanisms in the PV module. We adapt the CTM models in [8, 20] to incorporate effects of the frame and overlap widths. Changing the parameters of the frame can affect the module margin loss factor k_1 in case of a changed module area as described in Figure 5.

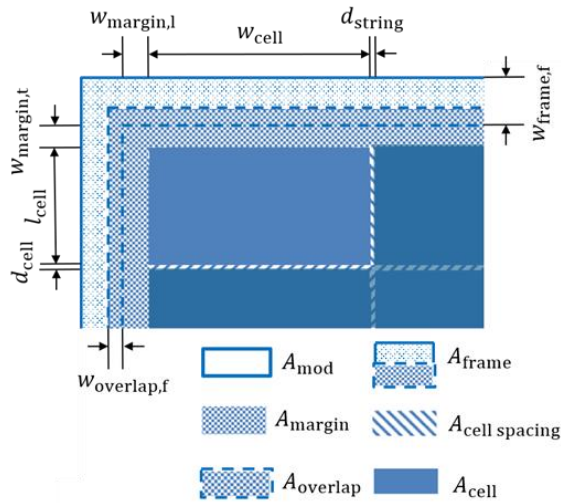


Figure 5: Outer and inner geometry and areas of PV module based on [21].

Furthermore, the frame design has impact on the cover coupling gain factor k_{11} due to changed module internal geometry shown in Figure 5 [20] and therefore optical coupling by light recycling, which is described in Figure 6.

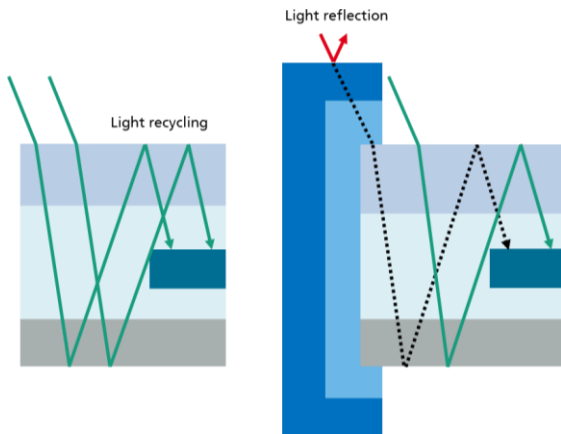


Figure 6: Schematic of the frame effect on the light recycling.

By calculating the additional module area due to the frame, we adjust the loss factor k_1 . By defining the frame/glass overlap width, we can calculate the shaded internal area. Shading reduces the short circuit current

change ΔI_{SC} used to calculate the gain factor k_{11} . The geometric frame overlap is used to correct the models of [11, 21].

2.3. Cost Analysis

Frames are typically manufactured by extrusion molding of aluminum ingots. Those ingots include the raw material price and the costs of manufacturing the billet used for further extrusion. Depending on the price for raw aluminum (06/2021 ~ 2 €/kg) [21], the ingots currently account for approximately 70% of the total frame costs. This stresses the importance of reducing frame weight without compromising mechanical stability. We calculate the cost share of the module frame by considering the material price for aluminum and a production share for the variations. The weight of the aluminum frame (kg/m) and the module circumference are taken from the dimensions used in mechanical and CTM analysis. We calculate the costs of the frame and the power loss due to frame shading and combine both to calculate the specific module costs C_{module} (€/Wp). A previously published study for module cost calculation is applied [10].

We calculate the costs of different frame designs based on individual aluminum consumption, which is directly related to the frame parameters. The manufacturing of the reference frame is calculated to account 2.34 €/piece and is assumed constant for all designs. The manufacturing costs of the frame, the framing process costs in module manufacturing (0.30 €) and the costs of the frameless module (62.00 €) are used with the frame material costs and the module power to calculate the module specific cost C_{module} .

2.4. Life Cycle Assessment (LCA)

The life cycle assessment is of great importance to evaluate the potential environmental impact caused by the module and especially the frame design. The carbon footprint or global warming potential GWP of the module, including the studied frames designs, is determined by using SimaPro Analyst v9.0 [22]. The PV foreground processes are based on previous work [12, 23], while background processes are based on Ecoinvent v3.7 database [24]. For the LCA, Germany is assumed as manufacturing location.

3. Results

The results of the different analyses for the various frame designs created from the parameters in Table 1 are presented separately within this section.

3.1. Mechanical analysis

Figure 7 exemplarily shows the deflection of the reference configuration at 2400 Pa as simulated by FEM. The maximum deflection d_{max} , occurring in the PV modules center, is 25.9 mm.

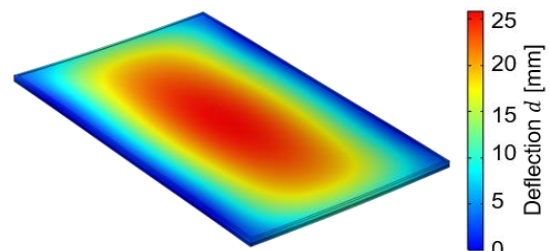


Figure 7: Deflection of the PV module of the reference frame at 2400 Pa push load simulated by FEM.

The maximum deflection d_{\max} of all investigated frame geometries is depicted in Figure 8. The variations show a deflection between 25.1 mm and 28 mm by changing the front and rear frame width from 10 mm and 12 mm to 20 mm and 20 mm, respectively. Compared to the reference frame, this is a decrease of 3% for the strongest frame design and an increase of 8.2% deflection for the weakest frame design. Comparing the influence of the front and rear width shows a stronger impact of the front width on the mechanical stability.

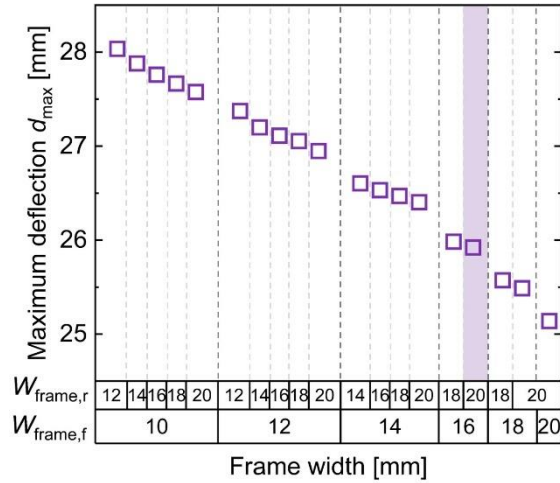


Figure 8: Maximum deflection d_{\max} of different frame designs at 2400 Pa push load. The reference module is marked in purple.

3.2. Cell-To-Module (CTM) Analysis

Since no light is photoconverted from the backside (glass-backsheet monofacial PV module), the rear side parameters of the frame do not affect module power or efficiency. Therefore, we only consider changing the front parameters of the frame for this part of the analysis. As the change in the overlap width in our approach equals the change in the frame width, the overall PV module area is constant. This leads to a constant module margin efficiency loss of -1.84% for all frame designs. In general, a smaller front frame overlap leads to a higher cover coupling gain factor k_{11} by allowing for more internal reflection on the white backsheet as described in Figure 6. In Figure 9, the PV module power and efficiency using different frame designs are shown.

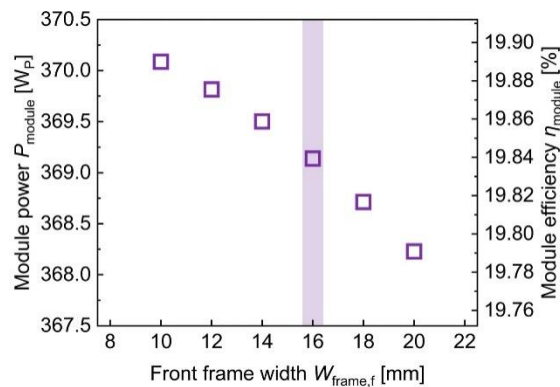


Figure 9: Power P_{module} and efficiency η_{module} of a monofacial 120-halfcell glass-backsheet PV module with different frame designs. The reference module is marked in purple.

It is recognizable that the module power increases due to higher internal reflection when decreasing the front frame width and thereby the overlap width. The module with the lowest front frame width and thereby the lowest overlap has the highest module power of 370.1 W_p and proportionately a module efficiency of 19.89%. This refers to the highest power gain due to cover coupling k_{11} of 7.85 W. Contrariwise, simulating the PV module with a 20 mm front frame width results in 1.86 W_p and 0.1% less module power and efficiency, respectively, due to lower cover coupling gain of 5.96 W. Compared to the PV module with the reference frame design, simulating the module with 10 mm front frame width results in a relative power and efficiency increase of about 0.26%.

3.3. Cost Analysis

We calculate the specific module cost C_{module} based on the different costs defined in the method part, the frame weight, and the PV module output power. Figure 10 shows an expected increasing trend of the module specific cost by increasing the frame width. This refers to the larger amount of aluminum used and to the reduced module power due to smaller coupling gains.

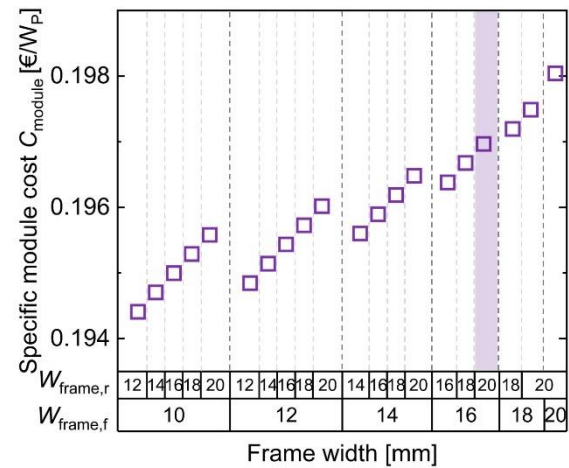


Figure 10: Specific module cost C_{module} using different frame designs. The reference frame design is marked in purple.

We find the module frame to have a share of approximately 10% of total module costs as shown in Figure 11.

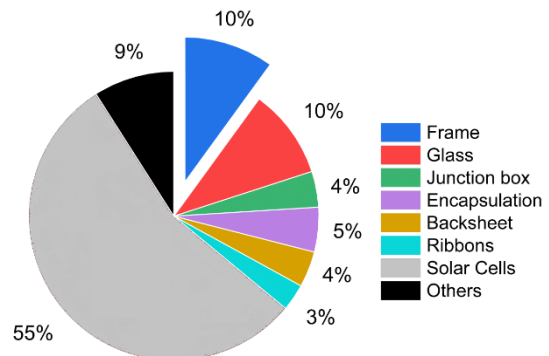


Figure 11: Cost of ownership share of a PV module with reference frame design.

The impact of margin shading due to frame overlap on specific module cost is small due to the small changes in module power. On the other hand, the frame mass has a larger impact on the specific module cost. Due to the cost shares in module and frame manufacturing we find that the module with the lowest specific cost has a 11.9% lower frame mass but leads to lower module costs of only 1.33%, which corresponds to around 1 €. Considering all designs, we find that a reduction of frame weight by about 9% reduces total module costs by 1%.

3.4. Life Cycle Assessment (LCA)

The results of the global warming potential GWP per kW_P nominal power of the reference module produced in Germany is shown in Figure 12.

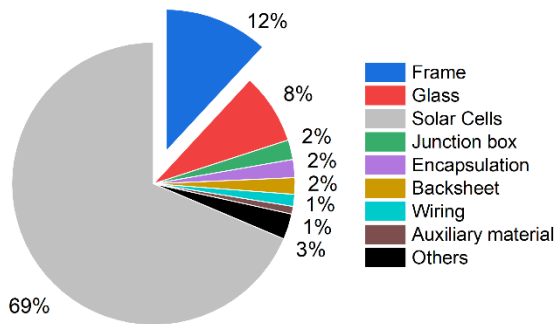


Figure 12: Global warming potential GWP share of PV module with the reference frame design.

Based on the results in Figure 12, the module frame has a significant impact on the global warming potential of the PV module. 31% of the total carbon footprint is related to the module materials, whereas the frame with 12% and the glass with 8% have the highest share of the emissions.

Hence, optimizing the frame design of PV modules offers a great potential to reduce the carbon footprint on the module as depicted in more detail in Figure 13.

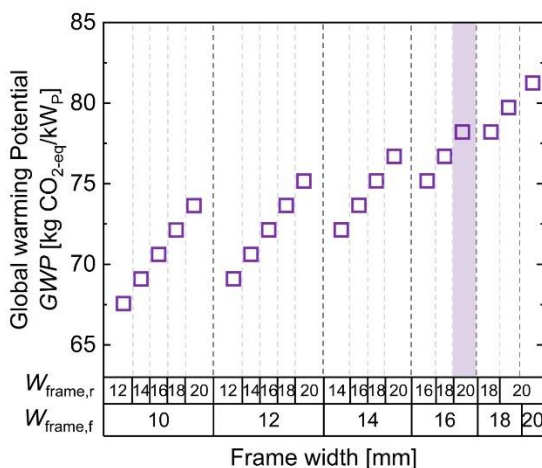


Figure 13: Global warming potential GWP of different frame designs. Reference frame is marked in purple.

It is obvious that decreasing the front and rear frame width (and thus the frame mass) has a significant influence on the CO_2 emissions. In comparison with the reference module, a CO_2 amount of up to 12%, corresponding to around 9 kg CO_{2-eq}/kW_P can be avoided when reducing front and rear frame widths to 10 mm and 12 mm

respectively due to the savings in aluminum. Furthermore, it can be observed that a reduction in the rear frame width is almost equally beneficial as minimizing the front frame width.

4. Discussion

The analyses show a potential to optimize the PV module frame. The results show that the mechanical stability is directly related to the frame height and weight which are relevant for costs and global warming potential. Therefore, the frame design optimization must be done with a focus on this aspect.

The results stress the necessity to reduce frame weight without compromising mechanical stability to reduce the module costs. An increase in overlap to achieve that is possible due to the comparatively small impact on the CTM power change. CTM analysis shows that the frame design has a small impact on the power of the PV module. Increasing the front frame width to 20 mm results in a decrement of 0.05%_{abs} in efficiency compared to the reference frame design. LCA analysis shows that an aluminum frame is large contributor to the module carbon footprint and that a reduction in frame weight is crucial for optimization.

Having a closer look to the results and combining them reveal that the frame design with 18 mm front and rear width has a lower cost as well as deflection and the same CO_2 footprint compared to the reference frame. Therefore, in a second step this design is further investigated in terms of weight reduction potential. We simulate ten different variations of this frame by FEM to identify the influence of different parameters. The variations do affect all aspects except the CTM analysis since the frame front and rear widths are constant. Figure 14 shows the change in maximum deflection and frame weight by applying the variations.

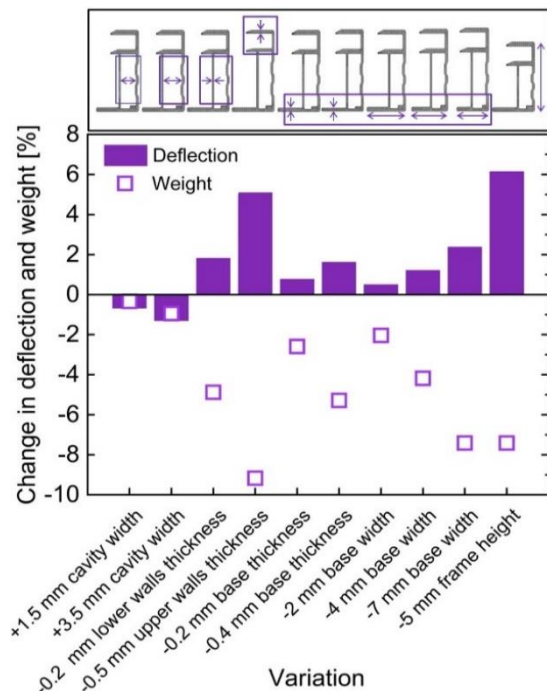


Figure 14: Change of maximum deflection and weight relative to the frame design with 18 mm front and rear width.

Enlarging the cavity decreases the deflection up to 1.3% and simultaneously the weight by 0.9%. All other changes lead to an increase of the deflection. The highest impact is due to decreasing the frame height (+6.1%) followed by decreasing the wall thickness of the upper frame part (+5.1%). Both also have a large impact on the weight (-7.4% and -9.2%). Decreasing the base thickness and length show a smaller impact on the deflection (between 0.8% and 2.5%) while having the same weight reduction potential as the frame height (2-7.4%). Therefore, we identify the cavity enlargement as well as a base thickness reduction as further optimization potential. However, choosing the frame design relies on manufacturer priorities regarding optimization.

5. Summary and Conclusion

By combining different simulation methods and analyses, we defined an approach for a holistic digital prototyping and optimization of the PV module frame. The simulation methods consist of mechanical FEM, CTM, COO and LCA analysis. With these methods, frame designs are investigated, and optimization potential is identified.

The highest optimization potential is identified for the frame front width followed. Figure 15 shows the reference design along with the variations that lead to a balanced optimization regarding mechanical stability, module power, costs, and carbon footprint.

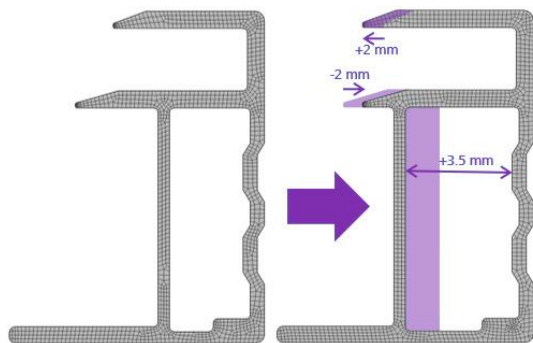


Figure 15: Reference frame design (left) and the variation with the highest optimization potential (right).

Compared to the PV module with the reference frame, the optimized design has a 2.6% lower deflection at 2400 Pa push load while saving 0.9% weight. The design reduces the PV module cost by 0.1% but also the PV module power by about 0.4 Wp. Around 1% of CO₂ emissions can be saved, which corresponds to 0.8 kg CO₂-_{eq}/kW_P due to around 30 g savings in aluminum. Other frame designs revealed an even higher reduction in cost and CO₂ footprint, with slight loss in mechanical stability. Therefore, the benefit of the presented holistic approach is that each aspect can be weighted individually to find a design optimized to the individual demand.

6. Acknowledgements

The authors acknowledge the funding of the work by the German Ministry of Economic Affairs and Energy under Grant No. 03EE1028A “CTS1000plus”.

7. References

- [1] M. A. Green, “Silicon photovoltaic modules: a brief history of the first 50 years,” *Progress in Photovoltaics*, vol. 13, no. 5, pp. 447–455, 2005, doi: 10.1002/pip.612.
- [2] A. Tummalieh, A. Pfreundt, and M. Mittag, “Trend Tracking of Efficiency and CTM Ratio of PV Modules: 37th European Specialist Conference and Exhibition,” 2020.
- [3] A. J. Beinert, P. Romer, M. Mittag, and J. Aktaa, “The Effect of Cell and Module Dimensions on thermomechanical Stress in PV Modules,” *IEEE J. Photovoltaics*, vol. 10, 2020.
- [4] A. J. Beinert, M. Ebert, U. Eitner, and J. Aktaa, “Influence of Photovoltaic Module Mounting Systems on the Thermo-Mechanical Stresses in Solar Cells by FEM Modelling,” 2016.
- [5] Y. Lee and A. A. Tay, “Stress Analysis of Silicon Wafer-Based Photovoltaic Modules Under IEC 61215 Mechanical Load Test,” *Energy Procedia*, vol. 33, pp. 265–271, 2013, doi: 10.1016/j.egypro.2013.05.067.
- [6] J. Y. Hartley *et al.*, “Effects of Photovoltaic Module Materials and Design on Module Deformation Under Load,” *IEEE J. Photovoltaics*, vol. 10, no. 3, pp. 838–843, 2020, doi: 10.1109/JPHOTOV.2020.2971139.
- [7] J. Schicker, Ch. Hirschl, and R. Leidl, “Effect of PV Module Frame Boundaries on Stresses in Solar Cells,” *Journal of Energy Challenges and Mechanics*, 2014, doi: 10.13140/2.1.3374.1441.
- [8] I. Haedrich, U. Eitner, M. Wiese, and H. Wirth, “Unified methodology for determining CTM ratios: Systematic prediction of module power,” *Solar Energy Materials and Solar Cells*, vol. 131, pp. 14–23, 2014, doi: 10.1016/j.solmat.2014.06.025.
- [9] Jibrán Shahid, Max Mittag, and Martin Heinrich, “A Multidimensional Optimization Approach to Improve Module Efficiency, Power and Costs,” 2018.
- [10] Fabian Fertig, Sebastian Nold, Nico Wöhrle, Johannes Greulich, Ingrid Hädrich, Karin Krauß, Max Mittag, Daniel Biro, Stefan Rein, Ralf Preu, “Economic feasibility of bifacial silicon solar cells,” *Progress in Photovoltaics*, 2016, doi: 10.1002/pip.2730.
- [11] V. Fthenakis and E. Alsema, “Photovoltaics energy payback times, greenhouse gas emissions and external costs: 2004–early 2005 status,” *Prog. Photovolt: Res. Appl.*, vol. 14, no. 3, pp. 275–280, 2006, doi: 10.1002/pip.706.
- [12] A. Müller, L. Friedrich, C. Reichel, S. Herceg, M. Mittag, D. H. Neuhaus, “A Comparative Life Cycle Assessment of Silicon PV Modules: Impact of Module Design, Manufacturing Location and Inventory,” *Solar Energy Materials and Solar Cells*, vol. 230, 2021.
- [13] A. Müller, K. Wambach, and E. Alsema, “Life Cycle Analysis of Solar Module Recycling Process,” *MRS Proc.*, vol. 895, 2005, doi: 10.1557/PROC-0895-G03-07.
- [14] A. Stoppato, “Life cycle assessment of photovoltaic electricity generation,” *Energy*, vol. 33, no. 2, pp. 224–232, 2008, doi: 10.1016/j.energy.2007.11.012.
- [15] A. Tummalieh, A. J. Beinert, C. Reichel, M. Mittag, and D. H. Neuhaus, “Holistic Design Optimization of the PV Module Frame: FEM, CTM, COO and LCA Analysis,” *Progress in Photovoltaics and Applications*, 2021.

- [16] A. J. Beinert and A. Masolin, "Enhancing PV Module Thermomechanical Performance and Reliability by an Innovative Mounting Solution: 37th European Photovoltaic Solar Energy Conference and Exhibition," 2020.
- [17] M. Mittag, T. Zech, M. Wiese, D. Bläsi, M. Ebert, and H. Wirth, "Cell-to-Module (CTM) Analysis for Photovoltaic Modules with Shingled Solar Cells: 44th IEEE Photovoltaic Specialists Conference," 2017.
- [18] M. Mittag, C. Reise, N. Wöhrle, R. Eberle, M. Schubert, and M. Heinrich, "Approach for a Holistic Optimization from Wafer to PV System: IEEE 7th World Conference on Photovoltaic Energy Conversion," 2018.
- [19] M. Mittag, A. Pfreundt, J. Shahid, N. Wöhrle, and D. H. Neuhaus, "Techno-Economic Analysis of Half Cell Modules - the Impact of Half Cells on Module Power and Costs," 2019.
- [20] I. Haedrich, D. C. Jordan, and M. Ernst, "Methodology to predict annual yield losses and gains caused by solar module design and materials under field exposure," *Solar Energy Materials and Solar Cells*, vol. 202, p. 110069, 2019, doi: 10.1016/j.solmat.2019.110069.
- [21] London Metal Exchange, *LME Aluminium*. [Online]. Available: www.lme.com (accessed: Jun. 13 2021).
- [22] *SimaPro Analyst v9.0: PRé Sustainability*. Accessed: Jun. 9 2021. [Online]. Available: <https://simapro.com/>
- [23] L. Friedrich, S. Nold, A. Müller, J. Rentsch, R. Preu, "Global Warming Potential and Energy Payback Time Analysis of Photovoltaic Electricity by Passivated Emitter and Rear Cell (PERC) Solar Modules," *IEEE Journal of Photovoltaics*, 2021.
- [24] *Ecoinvent database v.3.7*. [Online]. Available: <https://www.ecoinvent.org/>